Spike-Based High-Efficiency Data Compression Method for Intra-Body Galvanic Communication in Implantable Devices

Antonio Coviello*[1] Alice Cattelani*[1] Anna Vizziello[2] Pietro Savazzi[2] Atul Kumar[3] Maurizio Magarini[1]

[1] Department of Electronics Information and Bioengineering, Politecnico di Milano, Milan, Italy
[2] Department of Electrical, Computer and Biomedical Engineering, Università di Pavia, Pavia, Italy
[3] Department of Electronics Engineering Indian Institute of Technology (BHU) Varanasi, India
* Both authors contributed equally to this research
antonio.coviello@polimi.it

Abstract. Peripheral neuropathies represent a significant challenge in medicine, often inadequately addressed by conventional treatments. This work proposes a method for transferring information between implanted devices using galvanic currents. Diseases like nerve lesions causing facial palsy could be addressed by transmitting signals from a healthy to a damaged nerve via intra-body communication. A spike detection algorithm enables highly efficient data compression, with a compression factor up to 13000, extracting only the essential information required for nerve stimulation and minimizing transmission size. Experimental validation demonstrated effective communication up to 10 cm, with peak currents of 3 mA, compliant with ICNIRP safety guidelines. This innovative approach offers new prospects for restoring normal movements and improving the quality of life for affected patients.

Keywords: Electroneurographic signal (ENG), Galvanic Current, Intra Body Communication, Spike Detection.

1 Introduction

Peripheral neuropathies represent a significant challenge in the field of medicine, affecting millions of people globally. Peripheral neuropathies are among the most common neurological diseases with an incidence of 77 individuals per 100,000 inhabitants per year. They have a prevalence of 1 to 12% in all age groups with a peak of up to 30% in the elderly [1]. The market is expected to reach $9.7 billion by 2025 and the annual growth rate between 2020 and 2025 has been 9.1% [2]. Furthermore, the scientific community has shown more and more interest in studying these issues. The number of scientific publications has increased exponentially in recent years [3]. The motivation for this increase is the constant growth in the rate of occurrence of peripheral nerve injury (PNI) in the population. Lifestyle and the aging of the population are increasingly leading to this trend. Peripheral nerve injuries can have different triggering

factors, such as traumatic events, pathological conditions, work and sports accidents or injuries during daily activities. The recovery process of PNI is complex, characterized by a dedicated prognosis and a gradual recovery. This often results in impaired sensory and motor functions and, in some cases, permanent disability [4]. This not only decreases the overall quality of life of those affected but also amplifies the health burden on society. Despite advances in understanding the mechanisms underlying damage and regeneration, achieving complete functional recovery remains largely unsatisfactory for most patients. In fact, conventional treatments often fail to completely resolve related problems. In response to this challenge, the use of implanted devices emerges as a promising solution to address neuropathies. Only a strong collaboration between the world of medicine and the world of engineering will be able to permanently resolve currently incurable pathologies. One possible application concerns the use of implanted devices to treat pathologies such as facial paresis arising following a facial stroke. Studies suggest that facial paresis occurs in approximately 25% of ischemic or hemorrhagic stroke patients. The incidence of facial paresis after a stroke varies depending on the location of the stroke [5]. There are various therapeutic approaches for the management of post-stroke facial paresis. These include drug therapy, physical rehabilitation, and in some cases surgery. It is important to act immediately with rehabilitation to improve functional outcomes in patients with post-stroke facial paresis [6]. Advanced rehabilitation techniques, such as functional electrical stimulation and virtual reality-based therapy, are showing promising results in improving the recovery of patients with post-stroke facial paresis [7]. In the case of unsatisfactory recovery, it is possible to resort to implanted devices to guarantee recovery of functionality [8, 9]. An example that allows to show this application is reported in [10]. Using stable intracorporeal communication, such as that offered by the galvanic coupling (GC) technique, electroneurographic (ENG) signals could be recorded upstream of the lesion and sent to the compromised area. Intrabody communication (IBC) is more secure than other means of communication in terms of data protection. It also offers greater stability than other technologies such as Bluetooth, where communication can often be interrupted. Furthermore, data transmitted via galvanic current are properly preprocessed, as explained in this paper, real-time transmission could be ensured. This combination of security, stability and potential real-time application makes intrabody communication an innovative and promising solution to improve the quality of life of patients suffering from peripheral neuropathies and other medical conditions. In the case of partial facial paresis, signals could hypothetically be taken from the healthy side of the face through an implanted device that samples the signal from the facial nerve. The signals are then sent to the side affected by hemiparesis where a second device will proceed to carry out neuromodulation for motor restoration. For a better understanding of the application, we report Fig.1. By taking advantage of the facial symmetry of expressions, movement is restored on the pathological side. Only necessary information is transmitted between the two devices, minimizing the amount of data sent. To optimize communication, a spike detection approach is used, followed by various compression techniques to reduce the data size. Currently, there are no dedicated compression algorithms that use a spiking-based approach to compress ENG signals. Some examples of data compression

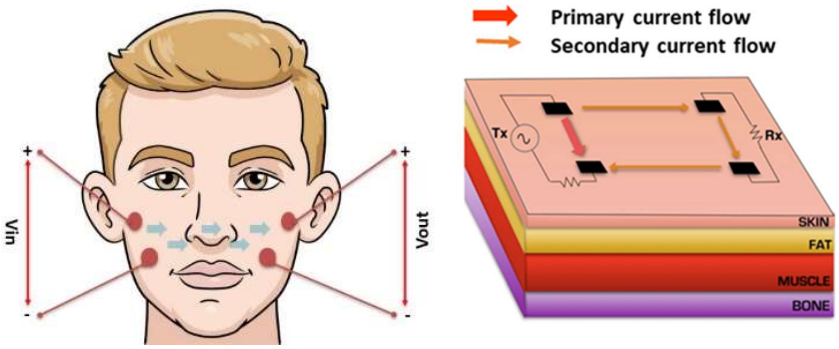

Fig. 1 Schematic representation of the GC communication mechanism used for facial paresis [11].

algorithm for ENG signal are reported in [12, 13]. This work focuses on signal processing to reduce data weight, enabling IBC experimentation in an efficient way. This paper introduces a novel thresholding algorithm for compressing ENG signals, adapted for intra-body communication, and provides an in-depth analysis of its effectiveness in spike detection and data reduction. Furthermore, it presents experimental validation of signal integrity for distances up to 10 cm and discusses the trade-offs inherent in the compression process. Through this approach, the goal is to develop an innovative solution to address peripheral neuropathies, offering new perspectives to improve quality of life of patients suffering from these conditions.

2 Intra Body Communication

Communication between devices using GC currents, known as intra-body communication, has attracted growing interest in various sectors, especially in medical applications. This method involves transmitting signals across or along the body surface, allowing the use of both superficial and implanted devices. It relies on the human body's ability to conduct electrical currents to send signals within the body [14, 15]. A voltage applied between the transmitter electrodes generates an alternating current that propagates through the body tissues until it reaches the receiver electrodes. This method is effective because the current can spread through body fluids, however, its efficiency depends on tissue dielectric properties, such as electrical conductivity and relative permittivity, and the frequency of the delivered current. The properties of biological tissues directly influence the propagation of electric current through the human body [16]. Indeed, the conductivity and permittivity of tissues are dependent on the delivery frequency. These values can influence the distribution of the electrical current and its ability to pass through different tissue layers. A shorter wavelength can make the signal more susceptible to phenomena such as scattering, especially if the wavelength becomes comparable to the size of body tissues [17]. Furthermore, high frequencies can lead to different behaviors than low frequencies in signal propagation through the body.

These parameters are crucial to understand how galvanic currents behave within the human body and are fundamental for the design and optimization of GC communication systems. For example, muscle tissue is known to be particularly efficient in transmission, while adipose tissue and bone are less effective in this process. The physiological characteristics of the patients must therefore be taken into consideration in the design phase. The optimal frequency range that should be used generally varies from 10 kHz to 100 MHz, with particular use of low frequencies to reduce current absorption and keep the local temperature low [18]. Power consumption is a critical parameter, especially in intracorporeal applications, where it is essential to minimize consumption to extend the operational life of the device. Reducing energy consumption can involve using less complex communication protocols, optimizing transmitter and receiver efficiency, and adjusting the device duty cycle. In GC technology, the energy needed to transmit data is equal to 1.28 nJ/bit. Current and voltage limits are strictly regulated to ensure safety. The reference standard for secure communication is IEEE 802.15.6 [19]. The data rate is another key factor, as it represents the transmission speed of the system. This strongly depends on the bandwidth, which in turn is influenced by the frequency and properties of the transmission medium, such as conductivity and attenuation of the signal. The complexity of the required modulation scheme and power constraints can further limit the data rate. In our application, it is possible to reach a maximum transmission speed of a few Mbit/s in the most optimal case [19]. Signal attenuation is related to loss of power as the signal propagates through body tissues. This phenomenon is influenced by various factors, including tissue composition and signal frequency. Modeling attenuation is essential to understand how the signal behaves during transmission. Generally, an attenuation of 65dB and an error of 1.8 mW/cm2 are observed using GC [19]. Transmission is also influenced by the connection distance, which represents the maximum distance within which communication remains reliable and efficient. Since each application may have different requirements in terms of minimum transmission path length, the link distance helps discriminate between the different techniques available. Specifically, the GC allows communication up to 15 cm maximum distance [19]. Finally, the concept of Maximum Permissible Exposure is crucial to ensuring the safety of intra-body applications. Defining the maximum level of safe exposure to electromagnetic fields, this parameter is determined experimentally and considers several factors such as frequency, power density and duration of exposure [19]. Compared to other IBC techniques, in GC technology the information is confined within the body, guaranteeing safety and privacy, with low signal dispersion, limiting any external interference. The simplicity of the system, which does not require external ground electrodes, leads to lower costs and allows the creation of implantable devices that can be positioned directly in the patient's region of interest, reducing physical and psychological discomfort [8]. The use of galvanic currents for communication offers numerous advantages, including low signal dispersion, protecting patient privacy and the possibility of using implantable systems. However, limitations such as transmission speed which is generally lower than other techniques such as Bluetooth, and sensitivity to electrode placement should be considered [20]. To solve this problem, it is possible to reduce the amount of data to be transmitted by using a preprocessing approach, as will be discussed in this paper.

3 Literature models

The absence of comprehensive alternatives has prompted the development of analytical models in scientific literature. In *vivo* experiments are often costly, and tissue phantoms do not fully replicate the variability of human tissue characteristics. Numerous studies have demonstrated the effectiveness of galvanic current communication in various applications. For example, [21] developed a finite element model for GC communication, simulating signal transmission through different body tissues. Furthermore, [22] conducted simulations using a multilayer body model to analyze the transmission of galvanic current in different regions of the body. An example of a complete electrical model for GC communication, reported in [23] Fig.2, would include a circuit for each individual tissue layer modeled as two-dimensional. This model incorporates impedance elements that represent different current paths, considering tissue composition, electrode contact impedance, voltage and current distribution. It thus offers detailed information on the behavior of galvanic current transmission through different body tissues. These analytical models form the basis for a more detailed understanding of IBC channels and allow an accurate evaluation of system performance. Furthermore, they introduce the possibility of considering the interaction between electrodes and tissues, providing a complete overview of signal propagation within the human body. Some preliminary studies have been conducted leveraging experimental data to evaluate the measured impulse response in *ex-vivo* chicken tissue and *in-vivo* human tissue, although in a limited frequency range up to 100 kHz [14]. Experimental results demonstrate that the channel is relatively flat in the frequency range of interest, thus offering the opportunity to simplify the design of an IBC transceiver.

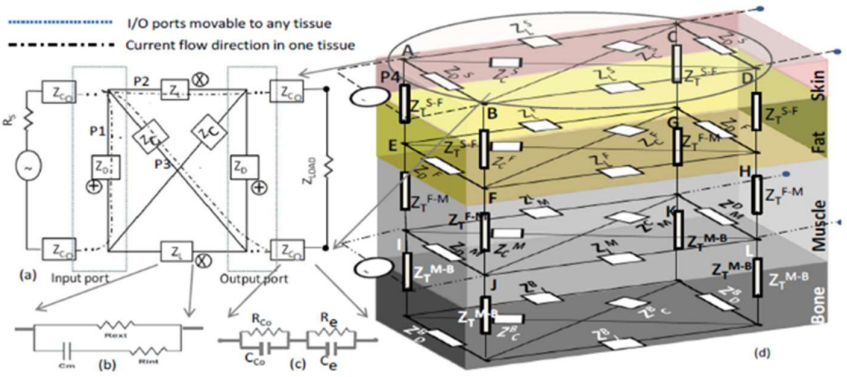

Fig. 2 Tri dimensional representation of a multilayered tissue model for GC IBC [23].

4 IBC Method

IBC represents a promising solution for enabling secure and efficient data transfer between implantable devices. However, the large amount of data generated by ENG signals poses significant challenges for real-time transmission and processing. This section outlines the methods developed in this work to address these challenges, focusing on signal compression and experimental validation of the communication setup. For the communication study, ENG data from the University of Newcastle were used [24]. Briefly, raw ENG signals have been taken from 3 different rats using different somatosensorial stimulation. Those includes proprioceptive signals of dorsiflexion (prop -30 -20 -10) and plantarflexion (prop +30 +20 +10), touch (100g, 300g) and pain (heel and outertoe). The signals are sampled at 30kHz, and the signal stimulation consists of several time alternation of stimulation (time ON) and rest (time OFF). Further data details are available in [8]. After initial preprocessing, the signal was reduced and transmitted from the source device to the receiver.

4.1 Experimental setup

To implement the hardware communication between the two devices, a scheme is reported in Fig. 3. Two laptop PCs and two external sound cards, the Creative Sound BlasterX G6, were used. Indeed, since GC frequency range (1 kHz - 100 MHz) includes the frequencies of the signals supported by the common sound cards, we exploit such feature to use such simple platform. This card combines a virtual 7.1 DAC, with maximum values of 130dB and 32-bit/384kHz, and an Xamp headphone amplifier. It connects directly to a laptop USB-C input via a cable and requires no additional power source. This device allows separation between the input and output channel for microphones and earphones. By connecting the card to a computer, you can set it as a transmitter (TX) or receiver (RX) for communication. To carry out the communication, each cable was connected to a sound card using the audio jack on one side and to two button superficial electrodes on the other. Each sound card is then connected to a PC while the electrodes are placed on a piece of chicken tissue to simulate biological conditions. Figure 3 illustrates how the setup would be applied to a human body in real-world

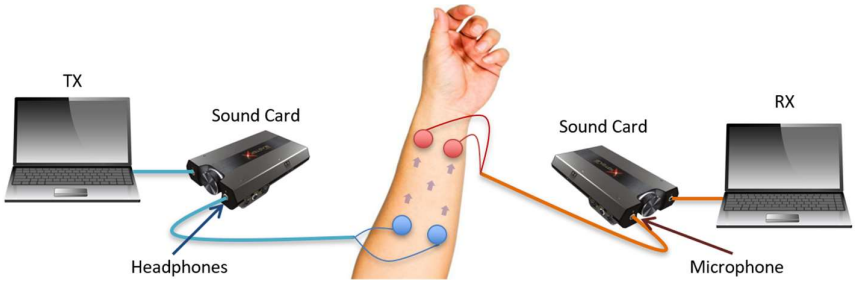

Fig. 3 Illustrative setup for GC communication on a human body [25].

scenarios. The surface button electrodes used are FIAB's PG10C, which, although designed for recording cardiac signals, are employed here for intra-body communication purposes. It is important to consider the specific characteristics of the headphone jack plug and how the audio cable carries the audio signal. A headphone cable, once connected, creates an electrical circuit that carries the audio signal from the source (the computer) to the headphones or any device connected to the other end of the cable (the electrodes). The cables used to transmit and receive the audio signal are characterized by TS connectors, which have only the tip and sleeve. These types of plugs are associated with unbalanced mono headphone signals. In the cable with this type of plug, there are two wires: the signal and the ground wire. The tip is connected to the signal wire while the sleeve serves as the ground wire. During the experiment, specific MATLAB code was run on each PC to transmit and receive the audio signal. Constant parameters ensure correct communication between devices. Some of these parameters are: 0.3 kHz carrier frequency, 96 kHz sample rate, 16-sample oversampling, and order 2 QAM modulation. Regarding the transmitter, after setting the parameters, the structure of the modulation filter is defined. The filter is a raised cosine FIR with R roll-off. The ENG signal is loaded, quantized and converted to binary using BPSK. The sequence is divided into preamble and main data. QAM modulation, oversampling, application of the FIR filter, and amplitude modulation with carrier frequency fc are then performed. Finally, the modulated audio signal is sent with the MATLAB audioplayer object. As regards the receiver, the parameters coincide with those of the transmitter. After setting the parameters and loading the original signal, the received signal is recorded using audiorecorder. It is demodulated, a SRRC FIR filter is applied and later downsampled. Carrier synchronization corrects any phase errors. The correlation technique aligns the signal in time, and a Wiener filter equalizes the signal, according to [18]. Different evaluation parameters such as BER, MSE bit, SNR and error probability for BPSK can be calculated to analyze the transmission efficiency. Before starting the transmission using galvanic technology, a careful evaluation of the value of the injected current was conducted to ensure the safety of the experimental setup, both for the application on the current skin and for any more complex future developments. To verify the safety of the experimental setup some preliminary assessments for the contact current are performed. To conduct these measurements, we used the Teledyne Lecroy Wavemaster 8330HD oscilloscope, an instrument capable of detecting voltage across a predetermined resistor. In our procedure, a section of the wire connected to the signal electrode was cut off and replaced with a 1 Ohm resistance. Through this resistance, we measured the voltage, which, according to Ohm's law (V=IR), allowed us to directly obtain the value of the current. On the transmitter side, the sound card was connected to the laptop via the USB-C port, while the wire, where the electrodes are attached, was connected to the headphone input of the sound card. Using the oscilloscope, we recorded the potential difference across the two exposed portions between the wire and the resistor as shown in Fig. 4. To test the worst-case scenario, the frequency on which the transmission was set was equal to 96 kHz and the volume level for the communication was set at 80% of the maximum, which represents the higher level used during the experiments. The safety limit was extracted from ICNIRP guidelines for contact currents and for our specific values was determined as 19.2 mA [26]. When the signal is transmitted, the

maximum value and the peak-to-peak value were obtained as 3 mA and 5.8 mA respectively. Therefore, both the values were largely compliant with the guidelines and our setup was labeled as safe and secure. Currently, the experimental setup uses non-implanted devices with surface electrodes applied to chicken tissue, limiting its direct applicability to implantable configurations. Future work will address this limitation by adapting the system for fully implantable scenarios. This approach ensured an accurate evaluation of the current injected into the system, providing a solid basis for the safety of the experiment and for future application development.

4.2 Data compression method

The pipeline used to carry out data reduction consists in the creation of an algorithm capable of reducing the information content of the ENG signal to its essential characteristics. Spikes represent the key points of the ENG signal to encode neural activity and are essential for transmission and classification. In this work, we developed a thresholding algorithm inspired by previous studies [27], specifically adapting it to improve spike detection and compression performance for intra-body communication

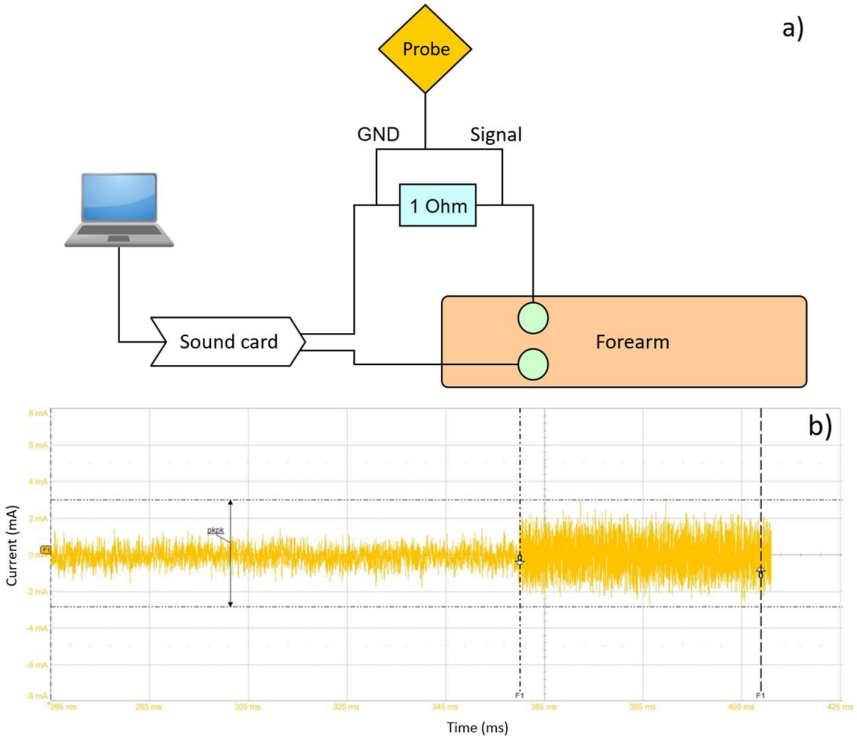

Fig. 4 a) Experimental setup for contact current registration; b) Correspondent result obtained.

applications. In particular, the individual action potentials (APs) are identified, which represent the building block of the signal. The identification of this activity is associated with the presence of nervous activity [8]. To evaluate the consistency of the algorithm, a downsampling of the signal at 15 kHz, 10 kHz and 5 kHz compared to the original 30 kHz was proposed, to analyze the performance at different frequencies. The algorithm was developed and executed on MATLAB R2023b. In order to identify the action potential, two thresholds are used, as reported in Fig. 5.a. Both thresholds are implemented in the positive and negative range to ensure a comprehensive detection of the spikes. The lower threshold is calculated by estimating the absolute median value of noise intrinsic to the signal (such as thermal noise).

The lower threshold is defined as follows:

$$\text{Lower Threshold Value} = 4 \times \frac{\text{Median}\ (|x|)}{0.6745} \tag{1}$$

where x represents the ENG signal at times of inactivity. The median value is calculated to exclude any noise from electronic equipment. This threshold will be much more accurate if it is possible to carry out the calculation only on non-activity traces. This guarantees to consider selectively the portion of the signal purely associated with noise. If the recordings include periods of activity alternating with periods of non-activity, as was the case in the six signals studied, this estimate will be less accurate. In case of inaccurate noise estimation, it is possible to reduce the factor 4 in Eq. (1) to lower values, such as 3.5 or 3. A lower threshold would allow to detect a higher number of spikes covered by noise. However, this approach implies a trade-off, as some of the detected spikes may be just noise. This choice requires a careful evaluation of the application context and the specific needs of the algorithm.

The upper threshold is formulated as follows:

$$\text{Upper threshold Value} = \text{N} \times \text{STD}(\text{x}) \tag{2}$$

Where x is the signal in which nervous activity is present, and N is a multiplier factor of the standard deviation. This factor is used to ensure that at least 99% of the AP population falls within the established thresholds. The statistical value associated with this measure varies between 4 and 6.5. Once the thresholds were determined, a first selection was made. However, included peaks can present problems. Assuming, as described in [27], that the duration of a single AP is 3.3 ms, no anomaly must be present for each peak within this time window. If, within the 3.3 ms range, the values exceed the upper threshold, they must be excluded as they are considered ripples of the noise to be canceled. Alternatively, if there are multiple peaks within the threshold in the window, only the largest should be selected. By carrying out this process, as shown in Fig. 5.b, it will be possible to correctly select the positions of the central peaks of the APs. The obtained spikes are as shown in Fig. 5c. Once the peaks of interest have been identified,

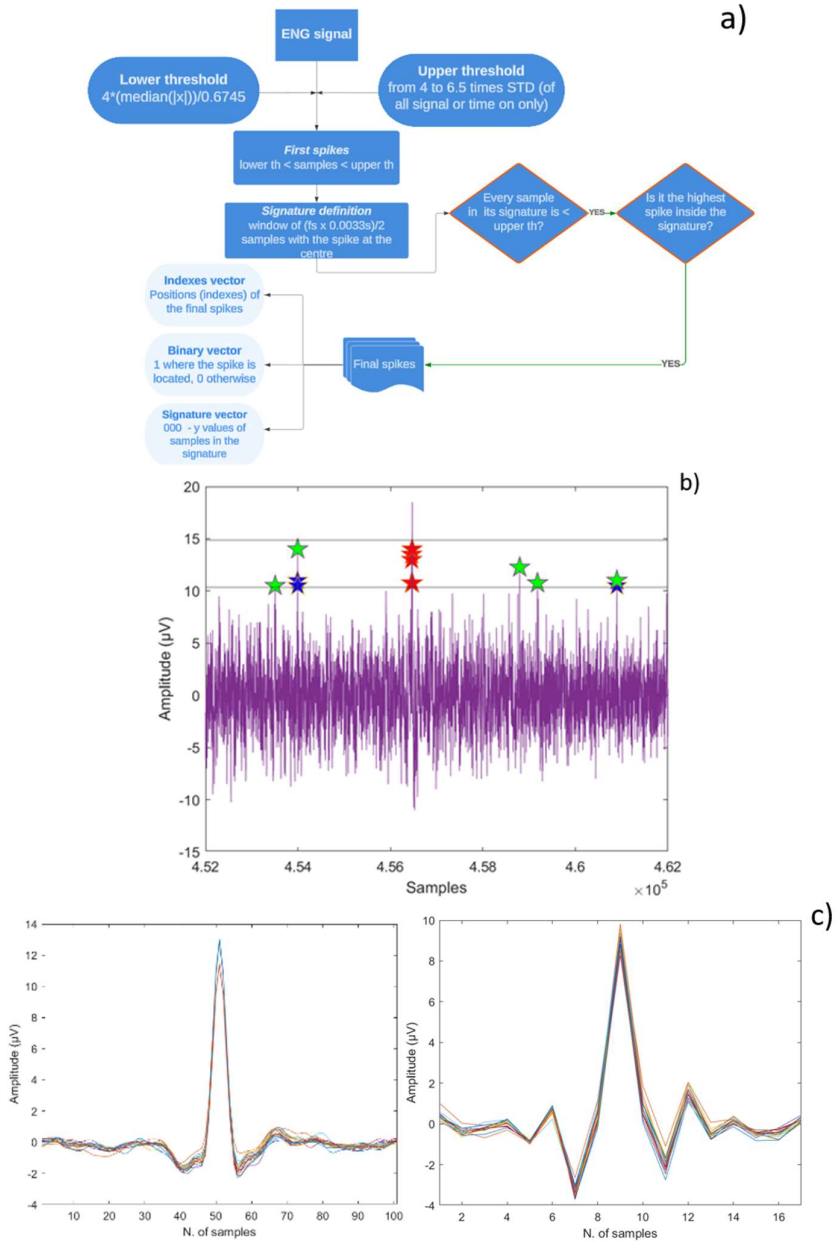

Fig. 5 a) Pipeline used for spikes data compression algorithm; b) Spike between upper and lower thresholds, red and blue are discarded while green are the correct ones; c) Shapes of the final extracted APs at 30 kHz and 5 kHz respectively.

it is possible to obtain three different outputs with different information content and length:

- Index vector: collects the positions of the indices of the central peak associated with the selected APs. It contains unsigned integers in ascending order.

- Zero count vector: A vector of the same length as the original, composed only of zeros and ones corresponding to the location of an AP. Since the probability of finding a one is very low compared to the total length of the signal, further processing is done to reduce the length. Starting from the created binary vector, it is possible to create a new encoding that indicates the position of the current zero and the number of zeros that follow it, thus reducing the final length of the vector.

- Signature vector: Contains the x(t) values of all temporal signatures associated with the final peaks. Each signature is sequentially separated by three zeros and the location of the central peak to distinguish them.

The compression process aims to reduce the length of the data while maintaining essential information, such as spikes, which are essential for classification. Unnecessary elements are eliminated. During communication the compressed signal remains intact and undistorted up to a distance of 10 cm between the electrodes, while greater distances require further analysis. The compression ratio (CR), as described in [12, 13], allows to quantify the different final signal length. We can define:

$$\mathrm{v} = [\mathrm{v}_1, \mathrm{v}_2, \dots, \mathrm{v}_\mathrm{n}] \tag{3}$$

as the vector containing with n samples of the original signal,

$$v' = [v'_1, v'_2, \dots, v'_m] \tag{4}$$

as a vector containing m samples after compression. We therefore define the length reduction factor as

$$\varepsilon = \frac{m}{n} \tag{5}$$

and the ratio between the size of the data types in bits (integer, double, float, …) as

$$\lambda = \frac{\text{size of v}'\text{data type [bits]}}{\text{size of v data type [bits]}} \tag{6}$$

Therefore, in the end the CR turns out to be:

$$\mathrm{CR} = \varepsilon \cdot \lambda \tag{7}$$

It is important to remember that the signal will have to be sent via electrodes. To distinguish the various values, they must fall within the available quantization of the device used. In the case of a 16-bit device, capable of providing up to 65 535 values, it is necessary to divide the data into packets respecting the maximum value supported by the device. Furthermore, it should be taken into consideration that with this code it is not possible to recover the original signal following compression, since much of the original ENG content has been discarded. However, the transformed signal can be used as encoding for classification algorithms, such as Spiking Neural Networks [28]. Finally, to obtain the optimal multiple of the standard deviation (STD) for the upper threshold, a statistical analysis was performed. By calculating the probability of finding a peak on the total signal (or only on the useful portion of interest), it is possible to estimate the optimal N value by identifying the plateau. This approach allows for the determination of a threshold that balances the inclusion of relevant spikes while minimizing the influence of noise. Probability values are calculated as follows:

$$P_1 = \frac{\#\, AP}{n} \tag{8}$$

5 Spike detection results and discussion

To accommodate the reduced throughput capacity of communication via galvanic currents, compression techniques based on the use of AP sensing have been implemented. First, the optimal value of the parameter N was determined, which acts as a multiplier to establish the optimal upper threshold. By setting N between 4 and 6.5, we observed the change in the number of peaks in the useful signal portions. As visible in Fig. 6 the tests carried out on three different rats' signals show that the number of peaks reaches a plateau for all stimulus categories and subjects after a value of N equal to 5.5. Interestingly, including the whole signal or only the parts with useful neural activity produces different probability results. This suggests that activity is indeed associated with useful periods and that the estimation works best when the inactive and active portions of the signal can be separated. The N value of 5.5 allows you to limit the loss of peak values, while ensuring a significant reduction in data load. Focusing on the different types of stimulation, as illustrated in Fig. 7, for nociceptive stimuli, the multiples range of 4 to 6.5 does not work correctly because the thresholds values are reversed. Interestingly, the code does not detect any peaks until the multiple reaches a value of 8.4. To address this issue, the lower threshold was set as the median of all lower thresholds, since the noise is essentially constant. Instead, for the higher thresholds, the highest was chosen. In a real-time application, in fact, it is not possible to implement multiple thresholds, but only one that can cover all the results. With these two thresholds, the number of APs selected per category is equally distributed for all stimulus categories, demonstrating the effectiveness of the method. An additional study was conducted by performing downsampling, as illustrated in Fig. 8. Length compression performance using 5 kHz resulted to be far less efficient than with 10 kHz and 15 kHz. Since spike

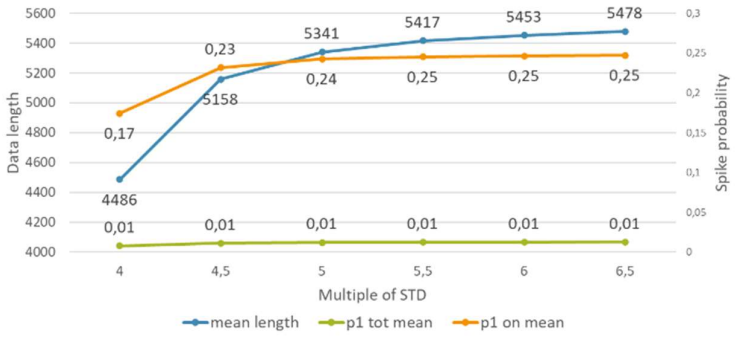

Fig. 6 Mean values of zero-output length, total spike probability (ON+OFF) and probability over time activity (ON) for proprioception ±30° at 30 kHz sampling.

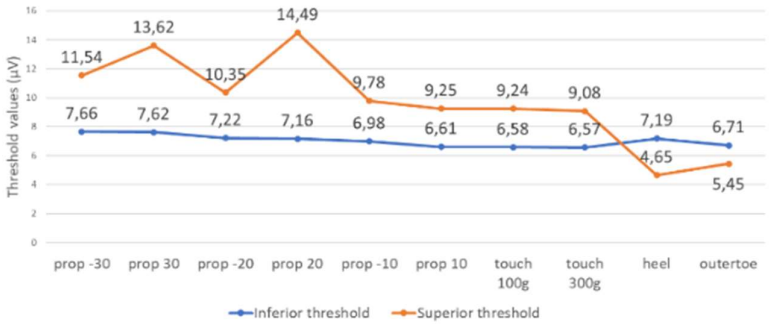

Fig. 7 Thresholds values for the different classes of signals for Animal 1 at 30 kHz.

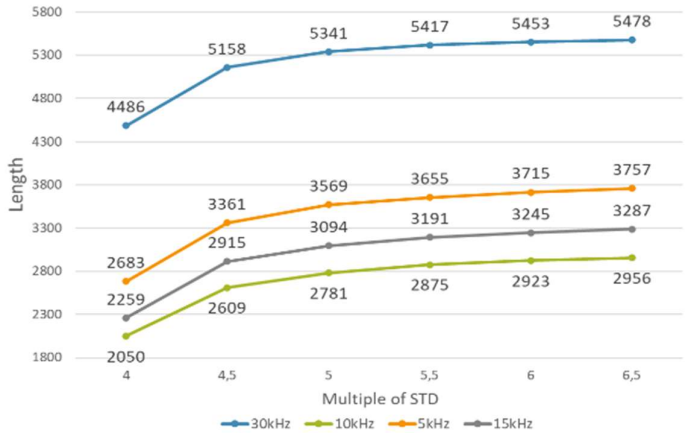

Fig. 8 Mean length of the zero-output for different sampling frequencies.

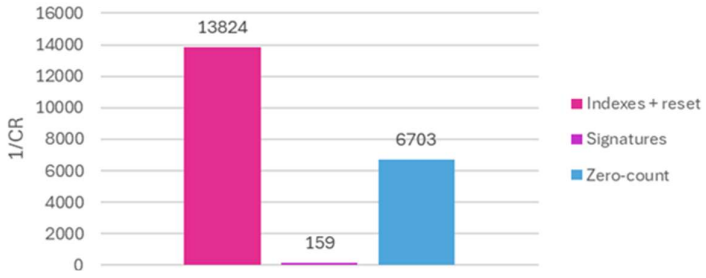

Fig. 9 Inverse of compression ratio for proprioception ±30° at 30 kHz.

detection relies on distinguishing between one sample and its neighbors, a reduced sampling rate leads to a binary vector with a higher frequency of spikes overall. For this reason, the sampling frequency that best optimized the reduction of the parameters was found to be 10kHz. These results allow us to set the parameters, specific for each subject, to implement and evaluate the effectiveness of the compression algorithms. Fig. 9 shows the inverse of the compression factor, which indicates the compression level achieved. A higher number indicates greater compression. The most effective algorithm in compressing signals was Index Vector, with a value of 13 824, followed by Zero Count Vector with a value of 6 703, and finally Signature Vector with a value of 159. These values are significantly higher compared to other compression algorithms implemented in [12, 13], where the maximum compression factor achieved was equal to 8. All algorithms can be considered effective, with greater attention to Index Vector in case you want to perform extreme compression or Signature Vector in case you want to preserve part of the information.

6 Conclusion

The use of galvanic currents for data communication between implantable devices offers significant potential advantages, as demonstrated in experiments on chicken tissue, and could enable safe and reliable transmission of information within the human body. While the proposed method demonstrates promising results, it is currently validated only for distances up to 10 cm, with further analysis needed for larger ranges. The compression algorithm prioritizes spikes, potentially discarding other relevant signal features. Moreover, in *vivo* validation and optimization for long-term energy efficiency remain open challenges. It would be interesting to explore the implementation of human IBCs in different body districts, supported by finite element simulations. The implementation of IBCs in areas such as arms, face, legs and abdomen would also allow to evaluate the efficiency of communication in relation to intrinsic variables between subjects, such as body mass index and constitution. This approach could expand the technology's applicability to various medical conditions, enhancing safety and enabling broader clinical use of IBC systems. Another promising area is the use of spiking neural

networks for the classification of data transmitted in real time. The use of galvanic currents for intra-body communication represents a rapidly evolving field of research with the potential to revolutionize the treatment of peripheral neuropathies and other medical conditions, paving the way for new therapies and significant improvements in patient care.

Acknowledgements

This study was partially supported by the European Union under the Italian National Recovery and Resilience Plan (NRRP) of NextGenerationEU, partnership on “Telecommunications of the Future” (PE00000001 - program “RESTART”) and by the AS23VARI19 ERASMUS+ project (KA171 CALL 2022 PROJECT) between the Polytechnic University of Milan and the Indian Institute of Technology (BHU) Varanasi.

References

1. Lehmann, Helmar C., et al. "Diagnosis of peripheral neuropathy." Neurological research and practice 2 (2020): 1-7.
2. Han, Ying, and Jun Yin. "Industry news: the additive manufacturing of nerve conduits for the treatment of peripheral nerve injury." Bio-Design and Manufacturing (2022): 1-3.
3. Zhang, Shiwen, et al. "Research hotspots and trends of peripheral nerve injuries based on web of science from 2017 to 2021: a bibliometric analysis." Frontiers in Neurology 13 (2022): 872261
4. Schreuders, Ton, et al. "Long-term outcome of muscle strength in ulnar and median nerve injury: comparing manual muscle strength testing, grip and pinch strength dynamometers and a new intrinsic muscle strength dynamometer." Journal of Rehabilitation Medicine 36.6 (2004): 273-278.
5. Laska AC, Hellblom A, Murray V, Kahan T, von Arbin M. Aphasia in acute stroke and relation to outcome. J Neurol Neurosurg Psychiatry. 2001;71(2):205-210.
6. Langhorne P, Bernhardt J, Kwakkel G. Stroke rehabilitation. Lancet. 2011;377(9778):1693-1702.
7. Cauraugh JH, Kim S. Two coupled motor recovery protocols are better than one: electromyogram-triggered neuromuscular stimulation and bilateral movements. Stroke. 2002;33(6):1589-1594.
8. Coviello, Antonio, et al. "Artificial Neural Networks-based Real-time Classification of ENG Signals for Implanted Nerve Interfaces." IEEE Journal on Selected Areas in Communications (2024).
9. Coviello, Antonio, et al. "Emerging peripheral nerve injuries recovery: advanced nerve-cuff electrode model interface for implantable devices." GCWOT'24 (2024): 1-7.
10. A. Vizziello et al., "An Implantable System for Neural Communication and Stimulation: Design and Implementation," in IEEE Communications Magazine, vol. 60, no. 8, pp. 74-79, August 2022, doi: 10.1109/MCOM.005.2101090.

11. A. Vizziello, P. Savazzi, and G. Magenes. "Electromyography data transmission via galvanic coupling intra-body communication link." Proceedings of the Eight Annual ACM International Conference on Nanoscale Computing and Communication. 2021.
12. Coviello, Antonio, et al. "Comparison of Data Compression Methods for Implanted Real-time Peripheral Nervous System." 2023 IEEE International Conference on Metrology for eXtended Reality, Artificial Intelligence and Neural Engineering (MetroXRAINE). IEEE, 2023.
13. Coviello, Antonio, et al. "Comparison of Imaging and Data Prediction Compression Methods for Implanted Real-Time Peripheral Nervous System." IEEE MetroXRAINE 2024. 2024. 1-6.
14. A. Vizziello, P. Savazzi, R. R. Guerra, and F. Dell'Acqua, "Experimental Channel Characterization of Human Body Communication Based on Measured Impulse Response," in IEEE Transactions on Communications, doi: 10.1109/TCOMM.2024.3370468.
15. Zhao, Jian Feng, et al. "A review on human body communication: Signal propagation model, communication performance, and experimental issues." Wireless Communications and Mobile Computing 2017 (2017).
16. Ahmed, Doaa, Georg Fischer, and Jens Kirchner. "Simulation-based models of the galvanic coupling intra-body communication." 2019 IEEE Sensors Applications Symposium (SAS). IEEE, 2019.
17. Seyedi, MirHojjat, et al. "A survey on intrabody communications for body area network applications." IEEE Transactions on Biomedical Engineering 60.8 (2013): 2067-2079.
18. A. Vizziello, P. Savazzi, G. Magenes, and P. Gamba, "PHY Design and Implementation of a Galvanic Coupling Testbed for Intra-Body Communication Links," in IEEE Access, vol. 8, pp. 184585-184597, 2020, doi: 10.1109/ACCESS.2020.3029862.
19. Tomlinson, William J., et al. "Comprehensive survey of galvanic coupling and alternative intra-body communication technologies." IEEE Communications Surveys & Tutorials 21.2 (2018): 1145-1164.
20. Quartana, Chiara, et al. "Wireless data transfer for Implanted Real-time Peripheral Nerve Interfaces." EAI BODYNETS 2023 2024. 2024. 1-20.
21. Chen, Zhi Ying, Yue Ming Gao, and Min Du. "Multilayer distributed circuit modeling for galvanic coupling intrabody communication." Journal of Sensors 2018 (2018).
22. Song, Yong, et al. "A finite-element simulation of galvanic coupling intra-body communication based on the whole human body." Sensors 12.10 (2012): 13567-13582.
23. Swaminathan, Meenupriya. Wireless Intra-Body Communication for Implantable and-Wearable Body Devices using Galvanic Coupling. Diss. Northeastern University, 2017.
24. Brunton, Emma, et al. "Identification of sensory information in mixed nerves using multi-channel cuff electrodes for closed loop neural prostheses." 2017 8th International IEEE/EMBS Conference on Neural Engineering (NER). IEEE, 2017.
25. https://it.creative.com/p/sound-blaster/sound-blasterx-g6.
26. Fields, Electromagnetic. "ICNIRP GUIDELINES." Health 17.9078/20 (2020): 0.

27. Koh, Ryan GL, Adrian I. Nachman, and José Zariffa. "Classification of naturally evoked compound action potentials in peripheral nerve spatiotemporal recordings." Scientific reports 9.1 (2019): 11145.
28. Coviello, Antonio, et al. "Neural network-based classification of ENG recordings in response to naturally evoked stimulation." Proceedings of the 9th ACM International Conference on Nanoscale Computing and Communication. 2022.